Peculiar catalytic properties of oxide glass-(ceramics) in epoxidation reactions

Jana Pisk, Sara Marijan, Teodoro Klaser, Petr Mošner, Ladislav Koudelka, Dominique Agustin, Željko Skoko, Luka Pavić

Peculiar catalytic properties of oxide glass-(ceramics) in epoxidation reactions

Jana Pisk,*[a] Sara Marijan,[b] Teodoro Klaser,[b] Petr Mošner,[c] Ladislav Koudelka,[c] Dominique Agustin,[d,e] Željko Skoko[f] and Luka Pavić*[b]

[a]*Department of Chemistry, Faculty of Science, University of Zagreb, Horvatovac 102a, 10000 Zagreb, Croatia.*
[b]*Division of Materials Chemistry, Ruđer Bošković Institute, Bijenička 54, 10000 Zagreb, Croatia.*
[c]*Department of General and Inorganic Chemistry, Faculty of Chemical Technology, University of Pardubice 53210 Pardubice, Czech Republic.*
[d]*LCC-CNRS (Laboratoire de Chimie de Coordination), 205 Route de Narbonne, BP44099, CEDEX 4, 31077 Toulouse, France.*
[e]*Department of Chemistry, IUT Paul Sabatier, Université Paul Sabatier, University of Toulouse, Av. G. Pompidou, CS20258, 81104 Castres, France.*
[f]*Department of Physics, Faculty of Science, University of Zagreb, Bijenička 32, 10000 Zagreb, Croatia.*

Highlights

- Glasses-(ceramics) from Na_2O-V_2O_5-(Al_2O_3)-P_2O_5-Nb_2O_5 system are explored as catalysts.
- Samples with ≥55 mol% V_2O_5 exhibit the highest activity and selectivity toward epoxide, in cyclooctene epoxidation.
- Tested oxidants, *tert*-butyl hydroxyperoxide in water and in decane provided good catalytic performance.
- The starting material can be recovered and reused in the 2nd run.
- The best catalytic performance is followed by high electrical conductivity.

Abstract

Glass-(ceramic) samples were prepared by melting mixtures of Na_2O-V_2O_5-(Al_2O_3)-P_2O_5-Nb_2O_5 in various molar ratios, and their catalytic performances were correlated to the structural, thermal, and electrical properties. The catalysts were tested in an

epoxidation reaction, with *tert*-butyl hydroxyperoxide in decane and water as oxidants. Samples containing the highest vanadium content are highlighted as the best catalysts (cyclooctene conversion 70-90 %), highly selective towards the desired epoxide (70-80%). At the same time, high electrical conductivity is observed with the value of ~10^{-5} S cm^{-1} @30 °C, which is 4-6 orders of magnitude higher in comparison to other studied samples.

Keywords

Phosphate-based glass-(ceramics), (ep)oxidation, catalysis, impedance spectroscopy, semiconductor inorganic material

Phosphate-based glassy- and glass-ceramic materials have generated increasing attention as promising contenders for solid electrolytes and/or electrode materials due to their favourable properties. Glass is a non-equilibrium, non-crystalline condensed state of matter exhibiting a glass transition with short-range order, but long-range disorder [1]. Glasses containing alkali oxides possess ionic conductivity, linked to the concentration and mobility of alkali ions. The mobility, in turn, is influenced by the disordered interaction between diffuse cations and the structural units of the glass. Furthermore, studies have demonstrated that glasses incorporating transition metal (TM) oxides, such as Fe_2O_3, V_2O_5, Nb_2O_5, WO_3, and MoO_3, exhibit electronic conductivity described by *small polaron hopping* mechanism, when TM exists in two oxidation states [2-4]. Such TM oxides are also known to serve as conditional formers, impacting the electrical properties not only through active participation in polaron transport but also by modifying the structure of the glass network [5-8].

Conversely, thermally induced or spontaneous crystallization of glass systems leads to the formation of composite materials, known as glass-ceramics [9-12]. It is well

known that nanomaterials usually have different properties than the corresponding bulk materials. These materials consist of a glassy matrix in which one or multiple crystalline phases are embedded, and, as such offer enhanced properties when compared to their glass counterparts [13-18].

Despite the extensive knowledge and research on the electrical properties of glass-ceramics, there is a significant limitation in the exploration of their catalytic applications. For example, bulk mixed metal oxides are commonly used in industry for various oxidation reactions, where catalytic reactions generally occur at active sites on the surface of heterogeneous catalysts [19]. It is well known that the specific activity of the active phase in a supported catalyst depends directly on its intrinsic activity and its specific surface area [20]. Bulk V−P−O catalysts are employed for the oxidation of *n*-butane to maleic anhydride [21]. Further, mixed metal oxide catalysts such as Mo−V−Nb−O and M−V−Nb−Te−O have proven efficiency in the oxidative dehydrogenation of propane to propylene and oxidation of propane to acrylonitrile, respectively [22,23]. Bulk vanadates have attracted attention due to their higher activity, selectivity, and greater stability at high temperatures compared to bulk mixed metal molybdates [24], specifically in the oxidation of methanol to formaldehyde. Nb−V mixed oxide catalysts were also used in the process of oxidative dehydrogenation of ethane and propane [25]. Additionally, ternary-system glasses, containing V_2O_5 were employed as catalysts for stearic and linoleic acid oxidation [26,27].

Building upon our previous expertise with vanadium, molybdenum or tungsten (TMO) molecular catalysts employed in the ep(oxidation) reactions, followed by great performances in terms of activity and selectivity [28-32], we decided to investigate the potential of glass-(ceramic)-based materials as catalysts in similar oxidation processes. Specifically, the utilization of TBHP in decane is anticipated to yield superior

conversion and selectivity outcomes in comparison with TBHP in a water media [33]. This approach represents an innovative extension of glass-(ceramics) applications, as they are primarily used as catalyst supports. A recent study by Stolar et al. [34] demonstrated that amorphous ZnCu-MOF-74 exhibited comparable selectivity to industrial $Cu/ZnO/Al_2O_3$ benchmarks for methanol formation, highlighting the advantages of employing amorphous materials as catalysts. Therefore, exploring glass-(ceramics) as direct catalysts offers a challenging and pioneering approach, expanding the scope of research in this field. Moreover, the melt quenching technique, a cost-effective and rapid method, proves invaluable in crafting these materials. It simplifies the preparation of large quantities, crucial for applications like catalysis and large-scale industrial use. Notably, its high reproducibility and the ease of fine-tuning material properties through simple compositional adjustments further enhance its appeal.

Based on the above-mentioned, a set of samples was prepared by mixing several precursors and melt-quenched to stainless-steel mould @RT thus leading to amorphous glasses and glass-ceramics Na_2O-V_2O_5-(Al_2O_3)-P_2O_5-Nb_2O_5 in different molar ratios (see **SI**, **Table 1**). The samples are labelled according to the amount of each oxide in the batch, e.g., 35Na-10V-35P-20Nb glass contains 35 mol% of Na_2O, 10 mol% V_2O_5, 35 mol% P_2O_5, and 20 mol% Nb_2O_5. The PXRD analysis (see **SI**, **Fig.S1** and **Table S2**) reveals the amorphous nature of all studied glasses, except samples 55V-10P-35Na and 70V-10P-20Na which are partially crystallized. Glass-ceramic 55V-10P-35Na contains crystal phase $Na_{1.164}V_3O_8$ (164514-ICSD) [35] embedded in an amorphous matrix, whereas in glass-ceramic 70V-10P-20Na, the presence of crystal phase $Na_{0.33}V_2O_5$ (239391-ICSD) [36] in a residual glass matrix is observed.

All samples were tested as catalysts using TBHP in decane as oxidant, *n*(catalyst) = 0.0018 mol. The three best catalysts were further tested under the following reactions:

ii) the use of TBHP in decane as oxidant, *n*(catalyst) = 0.0009 mol, and iii) the use of TBHP in water, *n*(catalyst) = 0.0009 mol. The ratio *n*(cyclooctene):*n*(oxidant) = 0.02mol:0.04 mol remained unchanged during each applied protocol. The first catalytic profile is presented in **Fig.1.**

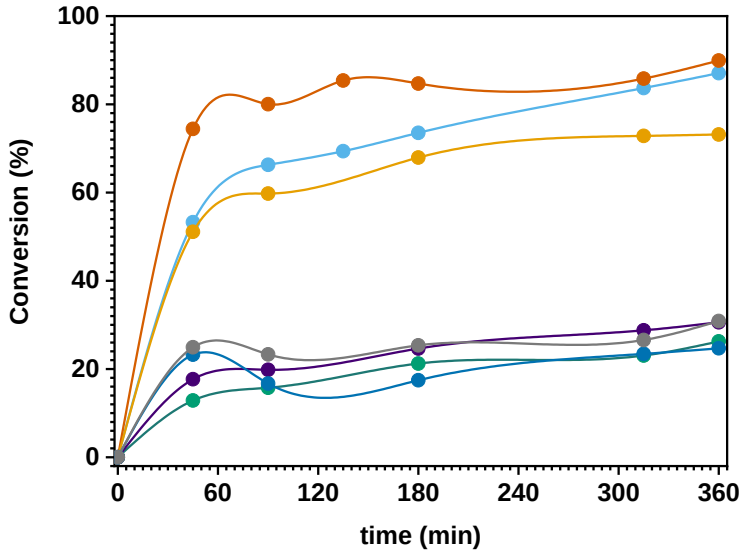

Fig.1. Converted cyclooctene vs. time with tested catalysts, from up to down: 70V-10P-20Nb orange curve, 70V-10P-20Na light blue curve, 55V-10P-35Na yellow curve, 35Na-10V-35P-20Nb grey curve, 35Na-45P-20Nb purple curve, 35Na-10Al-35P-20Nb green curve, and 35Na-25V-20P-20Nb dark blue curve. *n*(catalyst) = 0.0018 mol. TBHP in decane was used as the oxidizing agent. Temperature: 80 °C. The lines connecting data points are drawn as a guide to the eye. The error bars are at most of the order of the symbol size.

As seen, the most active catalysts are 70V-10P-20Nb, followed by 70V-10P-20Na and, 55V-10P-35Na, cyclooctene conversion ranging between 73 and 90%. Other tested catalysts did not show good catalytic profiles, cyclooctene conversion after 6 h of the reaction remaining between 26 and 30 %. Since the catalysts were partially soluble in the reaction media, we halved their quantity and compared the results with the initial catalytic protocol. Surprisingly, the activity of the samples 70V-10P-20Na and 55V-10P-35Na remained almost the same, while for the sample 70V-10P-20Nb conversion slightly decreased from 90 to 80% **(Fig.2)**.

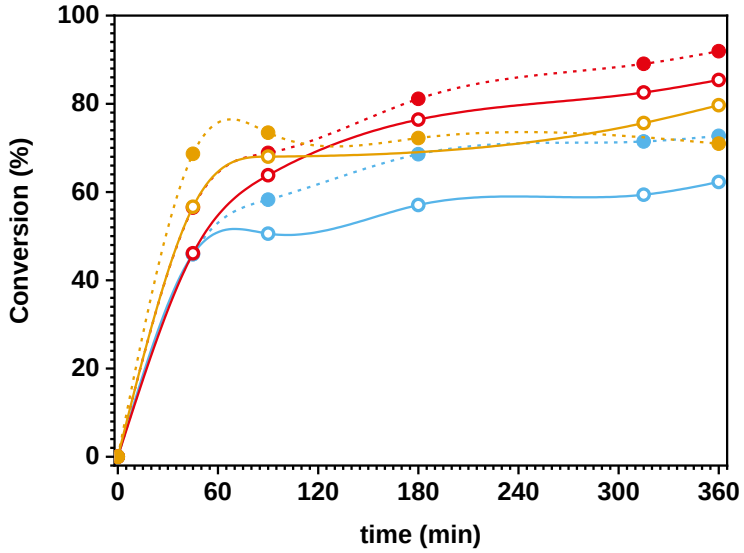

Fig.2. The influence of oxidizing agent. Converted cyclooctene vs. time with tested catalysts, from up to down: 70V-10P-20Nb yellow curve, 70V-10P-20Na red curve, 55V-10P-35Na blue curve. Full symbols present the reactions in which the oxidizing agent was TBHP in water, while empty symbols present the reactions in which the oxidizing agent was TBHP in decane. *n*(catalyst) = 0.0009 mol. Temperature: 80 °C. The lines connecting data points are drawn as a guide to the eye. The error bars are at most of the order of the symbol size.

In light of the obtained result, another oxidant, TBHP in water was tested, in order to analyse the influence of the oxide carrier, i.e. decane or water. As can be noticed from **Fig.2**, the activity of all three samples is better when the TBHP in decane is used as an oxidant, although the catalytic activities with TBHP in water show very good results, varying from 85 to 62%.

Furthermore, selectivity towards epoxide is very high for the samples 70V-10P-20Nb, 70V-10P-20Na, and 55V-10P-35Na (see **SI**, **Fig.S2**). The selectivity toward epoxide for the sample 70V-10P-20Na is the highest, 77%, no matter the catalytic protocol applied (amount of catalyst *vs* oxidant used). For the sample 70V-10P-20Nb, the selectivity is slightly higher in decane, 67% vs. 58% in water. On the other hand, the sample 55V-10P-35Na has the lowest selectivity between all three samples, no matter the choice of oxidant (around 60%). The epoxide selectivity for the samples 35Na-10V-35P-20Nb, 35Na-10Al-35P-20Nb, and 35Na-25V-20P-20Nb is around 40%, while for

the sample 35Na-45P-20Nb shows the lowest value, 28%. Due to the fact that the catalysts tested in the reaction with TBHP in decane, *n*(catalyst) = 0.018 mmol, were slightly soluble in the reaction media, it was possible to isolate them by filtration at the end of the reaction, in order to study their structural stability. As seen in **Fig.3**, the IR-ATR spectra of the catalyst before and after the reaction remain unchanged, showing the stability of the species. Since the catalysts 70V-10P-20Nb and 70V-10P-20Na showed the best catalytic activity, further reactions with the recycled catalysts were performed. It should be mentioned that more than 85% of the starting material could be recovered and reused in the 2nd run.

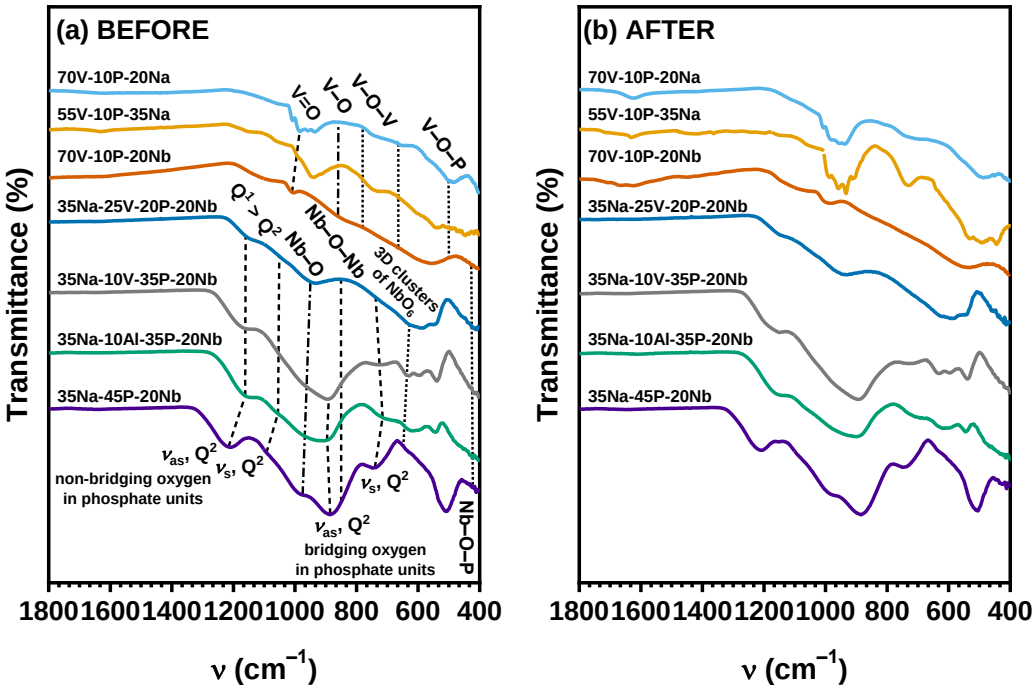

Fig.3. IR-ATR spectra of glass-(ceramic) samples from this study (a) before and (b) after the catalytic reactions. The IR spectra of all glass-(ceramic) samples remain unchanged before and after the catalytic reactions which indicates the stability of these materials under the given reaction conditions.

Catalytic profiles of the reaction with recycled catalysts are shown in **Fig.S3**, see **SI**. The catalytic activity of both catalysts is slightly lowered in the 2nd run, but is still quite high, 72% for the catalyst 70V-10P-20Nb and 67% for the catalyst 70V-10P-20Na. On

the other hand, selectivity towards epoxide, in the epoxidation reaction with TBHP in decane is around 70%, being still high.

The comparison of catalytic performance results between these materials and previously published ones involving a vanadium molecular catalyst is not straightforward and presents a challenging task due to the intricate nature of the systems. The best mononuclear vanadium molecular catalysts, in the reactions with 0,05 mol% [V] loading, and TBHP in water, provided the activity of 87% and a selectivity towards epoxide of 30% [28]. On the other hand, the dinuclear vanadium molecular catalyst, under the same condition, provided cyclooctene conversion of 98% and a selectivity parameter of 83% [29].

The obtained catalytic results can be correlated with the structural and electrical properties. The materials with the best catalytic properties are samples with the highest vanadium content, which supports the concept that vanadium-based materials are highly active as a catalyst in the epoxidation processes. Further, the samples 70V-10P-20Nb and 70V-10P-20Na show almost the same activity at the end of the reaction when using TBHP in decane with 0.0018 mol of catalyst. When diminishing the amount of catalyst to its half (0.009 mol), the difference in the activity becomes more pronounced, being mostly the same for 70V-10P-20Na and lower for the sample 70V-10P-20Nb. The observed behavior can be linked with structure, as abovementioned, the glass-ceramic 70V-10P-20Na consists of 57 wt% of the crystalline phase $Na_{0.33}V_2O_5$. embedded in an amorphous glass matrix (43 wt%), while the sample 70V-10P-20Nb is purely amorphous (see **SI**, **Fig.S1** and **Table S2**).

Raman spectra of the samples rich in vanadium, 70V-10P-20Nb and 70V-10P-20Na, closely resemble each other and are dominated by the signals corresponding to different vibrational modes of vanadate units connected into chains (see **SI**, **Fig.S4**),

possibly providing the positive catalytic behavior. The signal between 950–1050 cm^{-1} corresponds to symmetric stretching vibrations of the double V=O bond, whereas the broad signal between 600–950 cm^{-1} consists of overlapping signals describing vibrations of V–O and V–O–V in chains. In addition, the presence of a crystalline phase in the amorphous matrix for sample 70V-10P-20Na, and on the other hand Nb_2O_5 as network modifier for the sample 70V-10P-20Nb, seem to additionally contribute to the catalytic activity, resulting in similar catalytic profiles of both samples. The 55V-10P-35Na sample, featuring the crystal phase $Na_{1.164}V_3O_8$, also demonstrates a high cyclooctene conversion parameter. This is attributed to its rich vanadium loading, leading to a glass-ceramic network with vanadate units connected into chains (see **Fig.3** and **SI**, **Fig.S3**). Nevertheless, as anticipated, the catalytic activity is lower compared to the samples with a higher vanadium content.

Alongside catalytic testing, the electrical properties of all prepared samples were assessed using Solid-State Impedance Spectroscopy (SS-IS). A detailed analysis of the conductivity spectra (see **SI**, **Fig. S5**) and complex impedance plots (see **SI**, **Fig. S6**) along with Arrhenius plots (see **SI**, **Fig. S7**) is provided in the **SI**. The corresponding values of DC conductivity, σ_{DC}, @30 °C and activation energy for DC conductivity, E_{DC}, are given in **Table 1**.

Table 1. DC conductivity, σ_{DC}, activation energy, E_{DC}, pre-exponential factor, σ_0*

Sample	σ_{DC}@30 °C / S cm^{-1} ± 1%	E_{DC} / eV ± 1%	log(σ_0* (S cm^{-1} K)) ± 1%
70V-10P-20Na	1.34×10^{-5}	0.36	3.58
55V-10P-35Na	5.50×10^{-9}	0.45	2.09
70V-10P-20Nb	1.34×10^{-5}	0.32	3.49
35Na-10V-35P-20Nb	3.29×10^{-10}	0.65	4.39
35Na-25V-20P-20Nb	2.37×10^{-11}	0.71	4.16
35Na-10Al-35P-20Nb	3.44×10^{-9}	0.59	4.26
35Na-45P-20Nb	1.08×10^{-8}	0.58	4.70

The samples rich in vanadium show high DC conductivity, with a value of ~ 1×10^{-5} S cm^{-1} @30 °C, which is 4–6 orders of magnitude higher in comparison to other studied samples. The 55V-10P-35Na sample exhibits a lower value of DC conductivity, around 10^{-9} S cm^{-1}, related to a limited degree of crystallinity (14 wt% $Na_{1.164}V_3O_8$), hindering the formation of efficient conducting pathways through the crystalline grains. At the same time, the amorphous matrix becomes deficient in V^{4+}/V^{5+} pairs, resulting in lower DC conductivity.

The temperature dependence of σ_{DC} exhibits Arrhenius-like behaviour (see **SI**, **Fig.S7**) and it shows an increase with rising temperature, resembling the behaviour observed in semiconducting materials. The values of E_{DC}, determined from the slopes of $\log(\sigma_{DC})$ vs $1000/T$, fall within the range of 0.3–0.7 eV, aligning with reported values for sodium phosphate-based glasses containing niobium [37,38] and vanadium [39-42].

The observed trend in activation energy depending on composition aligns well with the different electrical conductivity mechanisms exhibited for these samples, as detailed in **SI**. Particularly, samples demonstrating pure and predominantly polaronic conductivity exhibit the lowest E_{DC} values, ranging from 0.32 to 0.45 eV, whereas samples with pure and predominantly ionic conductivity display E_{DC} values within the range of 0.58 to 0.71 eV.

Conclusions

To sum up, the best catalytic performances is, at the same time, followed by high electrical conductivity. The presented investigation provided multifunctional material that can be used at the same time as a catalyst and cathode material in batteries. To the best of our knowledge, the presented investigation is the first example of the correlation between structural, electrical, and catalytic properties of glass and glass-ceramics

systems. The obtained catalytic results highlight three catalysts, 70V-10P-20Nb, followed by 70V-10P-20Na and, 55V-10P-35Na as highly active and selective for cyclooctene epoxidation, under different conditions. It can be concluded that vanadium loading is crucial for catalytic activity and can be linked to the high electrical properties of the prepared materials, supporting the concept of electron migration between vanadium oxidation states (V^{5+}/V^{4+}). Further research will be directed toward the sample preparation and controlled crystallization of glass ceramics. We strongly believe that controlled and directed crystallization can obtain the non-soluble materials that should be fully recovered and recycled in the tested catalytic process.

Author Contributions

Conceptualization: J. P., L. P.; Data curation: J. P., S. M., L. P.; Formal Analysis: J. P., S. M., T. K., P. M., L. K., Ž. S., L. P.; Funding acquisition: J. P., L. P.; Investigation: J. P., S. M., T. K., P. M., L. K., Ž. S., L. P.; Methodology: J. P., D. A., Ž. S., L. P.; Project administration: J. P., L. P.; Resources: J. P., L. P.; Supervision: J. P., L. P.; Validation: J. P., S. M., L. P.; Visualization: J. P., S. M., L. P., Writing – original draft: J. P., L. P.; Writing – review & editing: J. P., L. P.

Declaration of Competing Interest

The authors declare that they have no known competing financial interests or personal relationships that could have appeared to influence the work reported in this paper.

Acknowledgments

This publication is based on COST Action Netpore (CA20126) work, supported by COST (European Cooperation in Science and Technology). This work is supported by

the Croatian Science Foundation, projects POLAR-ION-GLASS (IP-2018–01–5425) and "Young Researchers' Career Development Project – Training New Doctoral Students" (DOK-2021, S.M.). J.P. and Ž.S. acknowledge the support of project CIuK (Grant KK.01.1.1.02.0016) and CeNIKS (Grant No. KK.01.1.1.02.0013), respectively, co-financed by the Croatian Government and the European Union through the European Regional Development Fund-Competitiveness and Cohesion Operational Programme. J.P., S.M., and L.P. thank for the donation from the Croatian Academy of Science and Arts (HAZU) 2022. J. P and D. A acknowledge LCC CNRS and IUT Chem Dept are for equipment and chemicals for the catalysis experiments.

Notes and references

[1] E.D. Zanotto, J.C. Mauro, The glassy state of matter: Its definition and ultimate fate, J. Non-Cryst. Solids 471 (2017) 490–495.
[2] G. Austin, M. Sayer, Hopping conduction at high electric fields in transition metal ion glasses, J. Phys. C Solid State Phys. 7 (1974) 905–924.
[3] M. Sayer, A. Mansingh, Transport Properties of Semiconducting Phosphate Glasses, Phys. Rev. B 6 (1972) 4629–4643.
[4] I. G. Austin, N. F. Mott, Polarons in Crystalline and Non-crystalline Materials, Adv. Phys. 18 (1969) 41–102.
[5] A. Moguš-Milanković, K. Sklepić, H. Blažanović, P. Mošner, M. Vorokhta, L. Koudelka, , Influence of germanium oxide addition on the electrical properties of Li_2O-B_2O_3-P_2O_5 glasses, J. Power Sources 242 (2013) 91–98.
[6] A. Moguš-Milanković, K. Sklepić, P. Mošner, L. Koudelka, P. Kalenda, Lithium-Ion Mobility in Quaternary Boro–Germano–Phosphate Glasses, J. Phys. Chem. B 120 (2016) 3978–3987.
[7] M.P.F. Graça, M.A. Valente, M.G.F. Da Silva, The electric behavior of a lithium-niobate-phosphate glass and glass-ceramics, J. Mater. Sci. 41 (2006) 1137–1144.
[8] G. Tricot, H. Vezin, Description of the Intermediate Length Scale Structural Motifs in Sodium Vanado-phosphate Glasses by Magnetic Resonance Spectroscopies, J. Phys. Chem. C 117 (2013) 1421–1427.
[9] E.D. Zannoto, American Ceramic Society Bulletin 89 (2010) 19–27.
[10] W. Hölland and G. Beall, Glass-Ceramic Technology, John Wiley & Sons, New Jersey, 2nd edn. 2012.
[11] E. Le Bourhis, Glass: Mechanics and Technology, Wiley-VCH, Weinheim, 2008.
[12] P.W. McMillan, Glass–Ceramics, J.P. Roberts and P. Popper (Eds.), Non–Metallic Solids: A series of monographs, Vol. 1, 2. Ed., Academic Press, London, 1979.
[13] A. Moguš-Milanković, M. Rajić, A. Drašner, R. Trojko, D.E. Day, Crystallisation of iron phosphate glasses, Phys. Chem. Glasses 39 (1998) 70–75.

[14] A. Moguš-Milanković, K. Sklepić, Ž. Skoko, L. Mikac, S. Musić, D.E. Day, Influence of nanocrystallization on the electronic conductivity of zinc iron phosphate glass, J. Am. Ceram. Soc. 95 (2012) 303–311.
[15] L. Pavić, M.P.F. Graca, Ž. Skoko, A. Moguš-Milanković, M.A. Valente, Magnetic properties of iron phosphate glass and glass-ceramics, J. Am. Ceram. Soc. 97 (2014) 2517–2524.
[16] L. Pavić, Ž. Skoko, A. Gajović, D. Su, A. Moguš-Milanković, Electrical transport in iron phosphate glass-ceramics, J. Non-Cryst. Solids 502 (2018) 44–53.
[17] L. Pavić, J. Nikolić, M P.F. Graça, B.F. Costa, M.A. Valente, Ž. Skoko, A. Šantić, A. Moguš-Milanković, Effect of controlled crystallization on polaronic transport in phosphate-based glass-ceramics, Int. J. Appl. Glass Sci. 11 (2020) 97–111.
[18] L. Pavić, K. Sklepić, Ž. Skoko, G. Tricot, P. Mošner, L. Koudelka, A. Moguš-Milanković, Ionic conductivity of lithium germanium phosphate glass-ceramics, J. Phys. Chem. C 123 (2019) 23312–23322.
[19] O. Levenspiel, Chemical Reaction Engineering, Wiley, New York, 2nd edn., 465–466, 1975.
[20] J.F. Le Page, J. Cosyns, P. Courty, E. Freund, J.P. Franck, Y. Jacquin, B. Juguin, C. Marcilly, G. Martino, J. Miquel, J. Montarnal, A. Sugier, G. Van Landeghem, J. Limido Eds., Applied, Applied Heterogeneous Catalysis, Éditions Technip, Paris, 3–13, 1987.
[21] N. Ballarini, F. Cavani, C. Cortelli, S. Ligi, F. Pierelli, F. Trifiro, C. Fumagalli, G. Mazzoni, T. Monti, VPO catalyst for n-butane oxidation to maleic anhydride: A goal achieved, or a still open challenge?, Top. Catal., 38 (2006) 147-156.
[22] P. Botella, J. M. Lopez Nieto, A. Dejoz, M. I. Vazquez, A. Martinez-Arias, Mo–V–Nb mixed oxides as catalysts in the selective oxidation of ethane, Catal. Today 78 (2003) 507–512.
[23] W.D. Pyrz, D.A. Blom, N.R. Shiju, V.V. Guliants, T. Vogt, D.J. Buttrey, The effect of Nb or Ta substitution into the M1 phase of the MoV (Nb, Ta) TeO selective oxidation catalyst, Catalysis Today 142 (2009) 320–328.
[24] L.E. Briand, J.M. Jehng, L. Cornaglia, A.M. Hirt, I.E. Wachs, Quantitative determination of the number of surface active sites and the turnover frequency for methanol oxidation over bulk metal vanadates, Catal. Today 78 (2003) 257–268.
[25] K. Shimoda, S. Ishikawa, K. Matsumoto, M. Miyasawa, M. Takebe, R. Matsumoto, S. Lee, W. Ueda, Nb−V Mixed Oxide with a Random Assembly of Pentagonal Units: A Catalyst for Oxidative Dehydrogenation of Ethane and Propane, ChemCatChem. 13 (2021) 3132–3139.
[26] S.Y. Choi, B.K. Ryu, Nanocrystallization of vanadium borophosphate glass for improving the electrical and catalytic properties, J. Nanomater, 2015, 1. Article ID 201597, 9 pp.
[27] S.Y. Choi, B.K. Ryu, Effects of crystallization on the structural, electrical, and catalytic properties of $75V_2O_5–15B_2O_3–10P_2O_5$ glass, J. Non-Cryst. Solids 431 (2016) 112.
[28] J. Pisk, J.C. Daran, R. Poli, D. Agustin, Pyridoxal based ONS and ONO vanadium (V) complexes: Structural analysis and catalytic application in organic solvent free epoxidation, J. Mol. Catal. A: Chem. 403 (2015) 52–63.
[29] C. Cordelle, D. Agustin, J.-C. Daran, R. Poli, Oxo-bridged bis oxo-vanadium(V) complexes with tridentate Schiff base ligands $(VOL)_2O$ (L=SAE, SAMP, SAP): Synthesis, structure and epoxidation catalysis under solvent-free conditions, Inorg. Chim. Acta 364 (2010) 144–149.
[30] Jana Pisk, Dominique Agustin, Višnja Vrdoljak, Tetranuclear molybdenum(VI) hydrazonato epoxidation (pre)catalysts: Is water always the best choice?, Catal. Commun. 142 (2020) 106027.

[31] Silvija Mrkonja, Edi Topić, Mirna Mandarić, Dominique Agustin, Jana Pisk, Efficient Molybdenum Hydrazonato Epoxidation Catalysts Operating under Green Chemistry Conditions: Water vs. Decane Competition, Catalysts 11(7) (2021) 756.
[32] Višnja Vrdoljak, Jana Pisk, Dominique Agustin, Predrag Novak, Jelena Parlov Vuković, Dubravka Matković-Čalogović, Dioxomolybdenum(VI) and dioxotungsten(VI) complexes chelated with the ONO tridentate hydrazone ligand: synthesis, structure and catalytic epoxidation activity, New J. Chem. 38 (2014) 6176.
[33] T. Stolar, A. Prašnikar, V. Martinez, B. Karadeniz, A. Bjelić, G. Mali, T. Friščić, B. Likozar, K. Užarević, Scalable mechanochemical amorphization of bimetallic Cu−Zn MOF-74 catalyst for selective CO_2 reduction reaction to methanol, ACS Applied Materials & Interfaces 13 (2021) 3070–3077.
[34] M. Onoda, The crystal structures and quasi-one-dimensional electronic properties of $Ag_{1+x}V_3O_8$ and $Na_{1+x}V_3O_8$, J. Phys.: Condens. Matter. 16 (2004) 8957.
[35] A. Grzechnik, Y. Ueda, T. Yamauchi, M. Hanfland, P. Hering, V. Potapkin, K. Friese, Pressure-induced non-superconducting phase of β-$Na_{0.33}V_2O_5$ and the mechanism of high-pressure phase transitions in β-$Na_{0.33}V_2O_5$ and β-$Li_{0.33}V_2O_5$ at room temperature, J. Phys.: Condens. Matter. 28 (2015) 035401.
[36] T. Honma, M. Okamoto, T. Togashi, N. Ito, K. Shinozaki, T. Komatsu, Electrical conductivity of Na_2O-Nb_2O_5-P_2O_5 glass and fabrication of glass-ceramic composites with NASICON type $Na_3Zr_2Si_2PO_{12}$, Solid State Ionics 269 (2015) 19–23.
[37] S. Benyounoussy, L. Bih, F. Muñoz, F. Rubio-Marcos, M. Naji, A. El Bouari, Structure, dielectric, and energy storage behaviors of the lossy glass-ceramics obtained from Na_2O-Nb_2O_5-P_2O_5 glassy-system, Phase Transitions 94 (2021) 634–650.
[38] M. Wasiucionek, J. Garbarczyk, P. Kurek, W. Jakubowski, Electrical properties of glasses of the Na_2O-V_2O_5-P_2O_5 system, Solid State Ionics 70-71 (1994) 346–349.
[39] R.J. Barczyński, P. Król, L. Murawski, Ac and dc conductivities in V_2O_5-P_2O_5 glasses containing alkaline ions, J. Non-Cryst. Solids 356 (2010) 1965–1967.
[40] T.K. Pietrzak, W.K. Zajkowska, M. Wasiucionek, J.E. Garbarczyk, Observation of the metal-insulator transition of VO_2 in glasses and nanomaterials of MV_2O_5–P_2O_5 system (M = Li, Na, Mg), Solid State Ionics 322 (2018) 11–17.
[41] S. Kubuki, K. Osouda, A.S. Ali, I. Khan, B. Zhang, A. Kitajou, S. Okada, J. Okabayashi, Z. Homonnay, E. Kuzmann, T. Nishida, L. Pavić, A. Šantić, A. Moguš-Milanković, ^{57}Fe-Mössbauer and XAFS Studies of Conductive Sodium Phospho-Vanadate Glass as a Cathode Active Material for Na-ion Batteries with Large Capacity, J. Non-Cryst. Solids 570 (2021) 120998.